

Continuous-wave high-power rotational Raman generation in molecular deuterium

J. T. Green, D. E. Sikes, and D. D. Yavuz*

Department of Physics, 1150 University Avenue, University of Wisconsin at Madison, Madison, Wisconsin 53706, USA

**Corresponding author: yavuz@wisc.edu*

Received June 4, 2009; accepted July 2, 2009;
posted July 29, 2009 (Doc. ID 112289); published August 19, 2009

We report the generation of more than 300 mW of rotational Stokes output power in a CW Raman laser. The generation is achieved in low-pressure molecular deuterium inside a high-finesse cavity. © 2009 Optical Society of America

OCIS codes: 140.3550, 290.5910, 190.5650.

Since the pioneering work of Carlsten and colleagues [1–4] there has been a growing interest in CW Raman generation in molecular gases [5–7]. CW stimulated Raman scattering is achieved by placing the molecules inside a cavity with a high finesse at the pump and the generated wavelengths. Advances in high-reflectivity, ultralow loss dielectric coatings have allowed CW Raman laser thresholds as low as 1 mW and conversion efficiencies exceeding 65%. Since the generation is achieved inside a high-finesse cavity, the generated beams have very good temporal and spatial coherence properties. Both rotational and vibrational Stokes sideband generation has been reported with output powers typically in the 1 mW to 10 mW range [1,4]. Recently, Brasseur and colleagues have demonstrated 160 mW vibrational Stokes output power in molecular deuterium (D_2) [5].

In this Letter, we report an experiment that significantly advances the state of the art in CW stimulated Raman scattering. Specifically: (1) We report the generation of more than 300 mW of rotational Stokes output power in molecular D_2 . To our knowledge, this is the largest output power ever generated in a cavity-based gas-phase CW Raman laser. (2) We demonstrate this generation at a gas pressure of 0.1 atm, which is about 2 orders of magnitude lower than pressure values used in previous experiments. We operate in a regime with narrow Raman linewidths, and, as a result, the established CW molecular coherence in our experiment is more than 1 order of magnitude larger when compared with previous cavity-based systems.

We view our experiment as the first step for extending the technique of molecular modulation to the CW domain [8–10]. This technique relies on broadband Raman generation in the regime of maximum coherence. The key idea is to drive a molecular Raman transition with two slightly detuned laser beams and adiabatically prepare the molecules in a maximally coherent state. Under these conditions, a broad Raman spectrum is collinearly generated with phase matching playing a negligible role. By phase locking a subset of the generated spectrum, several recent experiments have demonstrated the synthesis

of the shortest laser pulses ever generated in the optical region of the spectrum [11,12]. These experiments have so far been performed with high-peak-power Q-switched lasers that have significant limitations. Extensions of the molecular modulation technique to the CW domain will require preparing molecules in a near maximally coherent state with CW driving laser beams [13]. To achieve this, operating at low gas pressures is critical to avoid pressure broadening of the Raman transition and to reduce phase mismatch between propagating laser beams.

Before proceeding, we also note the connection of this work to the recent beautiful experiment of Couny and coworkers who have demonstrated CW rotational Stokes output power of more than 2 W inside a hollow photonic crystal fiber at a gas pressure of 5 atm [14]. The key advantage of cavity-based approaches is the spectral purity of the generated radiation. In fiber experiments, the generated Stokes sideband has a bandwidth that is of the order of the linewidth of the Raman transition (typically about 500 MHz). In our work, however, we achieve kilohertz-level linewidths, since generation is achieved inside a high finesse cavity.

Figure 1 shows the setup of the experiment. To produce the desired high power pump laser beam, we start with an external-cavity diode laser (ECDL) at a wavelength of 1.55 μm . The ECDL is custom built with an optical power of 20 mW and a free running linewidth of about 0.5 MHz. After two Faraday isolators, the beam goes through an electro-optic modulator (EOM). The EOM puts 20 MHz phase modulation on the input beam, which is used to lock the laser to the high finesse cavity. We then amplify the beam with an erbium fiber amplifier. The amplifier is from IPG Photonics and produces a CW maximum output power of 30 W at an input power of 5 mW. The inputs and outputs of the amplifier are accessed through single-mode fibers. The 30 W output beam is linearly polarized with a measured polarization purity of 99% and has a beam size of 2 mm after the beam collimator. The beam then goes through an isolator and is coupled to the TEM_{00} mode of the high-finesse cavity (HFC) by using a mode-matching lens (MML). We

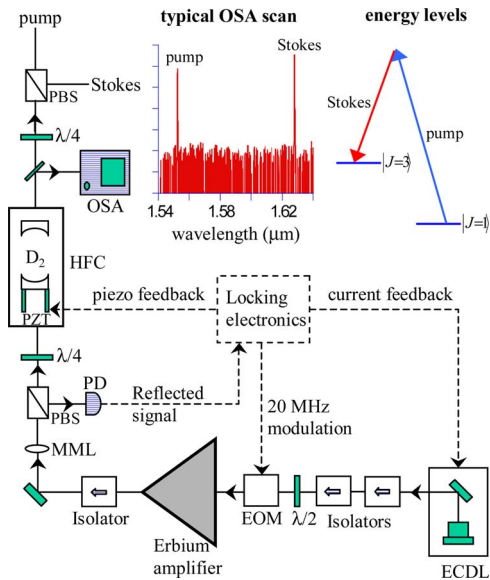


Fig. 1. (Color online) Setup of our experiment. The experiment starts with an external cavity diode laser at a wavelength of $1.55 \mu\text{m}$. After isolators, the laser beam goes through an electro-optic modulator that provides phase modulation at 20 MHz. The laser beam is then amplified to a high CW power level with the use of an erbium fiber amplifier. After the amplifier, the beam is linearly polarized with a maximum optical power of 30 W. The high power beam is then coupled to the cavity with the use of a mode matching lens. The plot shows a typical spectrum that we observe on an optical spectrum analyzer (the vertical scale is logarithmic). We observe Stokes sideband generation on the $|\nu=0, J=1\rangle$ to $|\nu=0, J=3\rangle$ rotational transition. ECDL, external-cavity diode laser; $\lambda/2$: half-wave plate; EOM, electro-optic modulator; MML, mode-matching lens, PBS, polarizing beam splitter; $\lambda/4$, quarter-wave plate; HFC, high-finesse cavity; PZT, piezoelectric transducer; PD, photodiode; OSA, optical spectrum analyzer.

convert the beam polarization to circular with a quarter-wave plate ($\lambda/4$) right before the cavity to maximize rotational sideband generation.

The HFC is placed inside a vacuum chamber that we fill with D_2 . The mirrors of the HFC are purchased from Precision Photonics, and they have low-loss, high-power, high-reflectivity coatings. The mirrors have a radius of curvature of 50 cm, and the spacing between the two mirrors is 27 cm, which gives a free spectral range of 555 MHz. One of the cavity mirrors is mounted on a piezoelectric transducer (PZT) to allow for slight adjustments of the cavity length. We measure the transmittance of the cavity mirrors to be 38 parts per million (ppm) at the pump and 277 ppm at the Stokes wavelength. The absorptive and scattering losses are at the 100 ppm level (quoted by the manufacturer) resulting in a cavity finesse of 22,764 for the pump and 8332 for the Stokes laser. We use the Pound–Drever–Hall technique to lock the pump laser to the TEM_{00} mode of the cavity [15]. For this purpose, we detect the reflected beam from the input cavity mirror with a photodiode and generate two separate feedback signals. The first feedback is sent directly to the diode of the ECDL laser modifying its current (fast feedback,

correction frequency range 50 Hz–500 kHz). The second feedback is sent to the PZT that controls the input cavity mirror making slight adjustments to the cavity length (slow feedback, correction frequency range dc–50 Hz).

Figure 2 shows the transmitted pump power through the cavity as a function of input power for an empty chamber (without D_2). The circulating intensity inside the cavity is calculated using the transmittance of the output cavity mirror (measured) and the cavity Gaussian mode radius of $W_0 = 331 \mu\text{m}$ (calculated). For an incident power of 25.4 W (measured right before the cavity) we measure an output transmitted power of 929 mW, which gives a peak circulating intensity of $14.1 \text{ MW}/\text{cm}^2$. The plot is roughly linear with a slight saturation suggesting that the damage threshold of the mirror coatings is significantly larger than the intensities achieved in our experiment. This is in agreement with the results of Meng and colleagues who have observed a CW laser damage threshold higher than $100 \text{ MW}/\text{cm}^2$ for these high quality optical coatings [16]. The transmitted power is substantially lower than the incident power due to the following reasons: (1) The absorptive and scattering losses of the cavity mirrors at the pump wavelength are larger than mirror transmission loss. (2) The finite bandwidth of the locking servo electronics results in imperfect spectral narrowing of the ECDL. (3) The spatial mode matching of the input laser beam to the cavity mode is not perfect.

When we fill the chamber with molecular D_2 , we observe opposite circularly polarized Stokes sideband above the lasing threshold. The lasing occurs on the $|\nu=0, J=1\rangle$ to $|\nu=0, J=3\rangle$ rotational transition at a transition frequency of 297 cm^{-1} (8.9 THz). The pump beam at a wavelength of $1.55 \mu\text{m}$ produces a Stokes beam at a wavelength of $1.63 \mu\text{m}$. After the

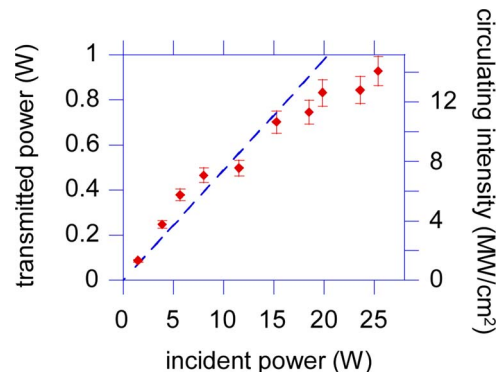


Fig. 2. (Color online) Transmitted pump power through the cavity as the incident power is varied for an empty chamber (without D_2). The dashed line is a linear fit to the first six data points. The intracavity circulating intensity is calculated by using the measured mirror transmittance and the transverse cavity mode size. We achieve a circulating intensity of $14.1 \text{ MW}/\text{cm}^2$ for an incident power of 25.4 W. The plot does not show severe saturation indicating a mirror coating damage threshold substantially larger than $14.1 \text{ MW}/\text{cm}^2$. The transmitted power is much lower than the input power owing to a variety of reasons including scattering and absorptive losses of the mirrors and imperfect servo electronics. See text for details.

cavity, we separate out the pump and the Stokes beams with the use of a quarter wave plate and a polarizing beam cube. Figure 3 shows the transmitted power in the pump and the Stokes beams as a function of incident pump power for a D_2 pressure of 0.1 atm. We observe a laser threshold of 1.1 W, and for an incident pump power of 25.4 W we generate 321 mW of output Stokes beam.

We have estimated the expected Raman gain coefficient by using the matrix elements in the Lyman and Werner bands from the work of Allison and Dalgarno [17]. By using the circulating intensity data of Fig. 2, we estimate a Raman laser threshold of 223 mW for the incident pump power, assuming that the Stokes radiation is emitted at the Raman gain peak. However, Fig. 3 indicates about a factor of five larger laser threshold. The discrepancy is likely caused by the following reasons: (1) imperfect frequency overlap of the cavity Stokes lasing mode with the Raman gain peak, and (2) the degradation of cavity locking due to thermal focusing effects when we

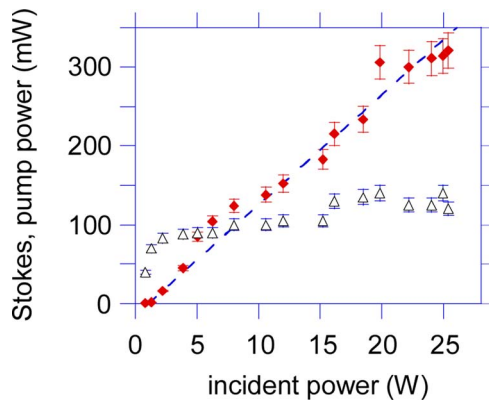


Fig. 3. (Color online) Transmitted pump power (triangles) and the generated Stokes power (squares) as a function of the incident pump power at a D_2 pressure of 0.1 atm. The dashed line is a linear fit to the Stokes power data points. For an incident power of 25.4 W we generate 321 mW of output Stokes beam. To our knowledge, this is the largest output power ever generated in a cavity-based gas-phase CW Raman laser. The observed lasing threshold is 1.1 W for the incident pump beam, which is about a factor of 5 higher than the theoretical estimate. We attribute the discrepancy to various effects, some of which may be overcome in the future by technical improvements.

fill the chamber with D_2 . As demonstrated by Carlsten and colleagues, cavity lock degradation can be minimized by careful considerations on the lock circuit, which we plan to implement in the near future [18].

We thank Nick Proite for his assistance with the experiment. This work is supported by the National Science Foundation (NSF) and the University of Wisconsin at Madison.

References

1. J. K. Brasseur, K. S. Repasky, and J. L. Carlsten, *Opt. Lett.* **23**, 367 (1998).
2. J. K. Brasseur, P. A. Roos, K. S. Repasky, and J. L. Carlsten, *J. Opt. Soc. Am. B* **16**, 1305 (1999).
3. L. S. Meng, P. A. Roos, K. S. Repasky, and J. L. Carlsten, *Opt. Lett.* **26**, 426 (2001).
4. L. S. Meng, P. A. Roos, and J. L. Carlsten, *Opt. Lett.* **27**, 1226 (2002).
5. J. K. Brasseur, R. F. Teehan, P. A. Roos, B. Soucy, D. K. Neumann, and J. L. Carlsten, *Appl. Opt.* **43**, 1162 (2004).
6. K. Ihara, C. Eshima, S. Zaitzu, S. Kamitomo, K. Shinzen, Y. Hirakawa, and T. Imasaka, *Appl. Phys. Lett.* **88**, 074101 (2006).
7. S. Zaitzu, H. Izaki, and T. Imasaka, *Phys. Rev. Lett.* **100**, 073901 (2008).
8. A. V. Sokolov, D. R. Walker, D. D. Yavuz, G. Y. Yin, and S. E. Harris, *Phys. Rev. Lett.* **85**, 562 (2000).
9. J. Q. Liang, M. Katsuragawa, F. Le Kien, and K. Hakuta, *Phys. Rev. Lett.* **85**, 2474 (2000).
10. T. Suzuki, M. Hirai, and M. Katsuragawa, *Phys. Rev. Lett.* **101**, 243602 (2008).
11. M. Y. Shverdin, D. R. Walker, D. D. Yavuz, G. Y. Yin, and S. E. Harris, *Phys. Rev. Lett.* **94**, 033904 (2005).
12. W. Chen, Z. Hsieh, S. Huang, H. Su, T. Tang, C. Lin, C. Lee, R. Pan, C. Pan, and A. H. Kung, *Phys. Rev. Lett.* **100**, 163906 (2008).
13. D. D. Yavuz, *Phys. Rev. A* **76**, 011805(R) (2007).
14. F. Couny, F. Benabid, and P. S. Light, *Phys. Rev. Lett.* **99**, 143903 (2007).
15. R. W. P. Drewe, J. L. Hall, F. V. Kowalski, J. Hough, G. M. Ford, A. J. Munley, and H. Ward, *Appl. Phys. B* **31**, 97 (1983).
16. L. S. Meng, J. K. Brasseur, and D. K. Neumann, *Opt. Express* **13**, 10085 (2005).
17. A. C. Allison and A. Dalgarno, *At. Data* **1**, 289 (1970).
18. J. C. Biefang, W. Rudolph, P. A. Roos, L. S. Meng, and J. L. Carlsten, *J. Opt. Soc. Am. B* **19**, 1318 (2002).